Uniaxial ferromagnetism in $NiZrF_6 \cdot 6H_2O$

M. Karnezos, D. L. Meier, and S. A. Friedberg
Physics Department, Carnegie-Mellon University, Pittsburgh, Pennsylvania 15213
(Received 15 August 1977)

$NiZrF_6 \cdot 6H_2O$ crystallizes in the trigonal $NiSnCl_6 \cdot 6H_2O$ structure with one trigonally distorted $[Ni(H_2O)_6]^{2+}$ complex per unit cell. We have measured $\chi_\parallel$ and $\chi_\perp$ for this salt between 0.05 and 4.2 K and C_p in zero field and in $H_\parallel = 2000$ Oe between 0.09 and 4.2 K. The susceptibilities are those of a uniaxial ferromagnet with the easy axis along the trigonal direction and $T_C \approx 0.16$ K. $C_p(H=0)$ exhibits a sharp cooperative peak at $T_C = 0.164 \pm 0.002$ K and a Schottky anomaly with $C_{max}/R \approx 0.24$ and $T_{max} \approx 1.5$ K. Thus, the ${}^3A_{2g}$ ground state of $[Ni(H_2O)_6]^{2+}$ is split into a lower doublet and an upper singlet separated by $\sim 3k$ and the ionic moments are Ising-like near T_C. $C_p(H_\parallel = 2$ kOe) shows two overlapping rounded anomalies. The data are well described by an Oguchi model in which pairs of spins are treated exactly and their interaction with the rest of the crystal is represented by a mean field. The pair Hamiltonian is $\mathcal{H} = D(S_{zi}^2 + S_{zj}^2) - 2J\vec{S}_i \cdot \vec{S}_j + g\mu_B(\vec{S}_i + \vec{S}_j) \cdot \vec{H}_{eff}$ where $S_i = S_j = 1$, $\vec{H}_{eff} = \vec{H}_{app} - [2J(z-1)/Ng^2\mu_B^2]\vec{M}$, $D/k = -3.14$ K, $g = 2.33$, and $zJ/k = +0.084$ K. Dipolar coupling accounts for about one-fourth the spin interaction energy in this salt and appears to give it the mean-field-like character of a dipolar Ising ferromagnet.

INTRODUCTION

Nickel chlorostannate hexahydrate, $NiSnCl_6 \cdot 6H2O$, was shown by Pauling[1] many years ago to crystallize in a trigonal structure belonging to the space group $R\bar{3}$. The rhombohedral unit cell ($a = 7.09$ Å and $\alpha = 96°45'$) contains a single $[Ni(H_2O)_6]^{2+}$ complex which is distorted along a trigonal axis parallel to that of the crystal. Interestingly enough, the ground state of this complex was first studied, not in the chlorostannate, but in another of a large group of compounds of Ni^{2+} that crystallize in the same structure, namely, $NiSiF_6 \cdot 6H_2O$, for which $a = 6.26$ Å and $\alpha = 96°6'$. Magneto-optical,[2,3] paramagnetic resonance, magnetic, and thermal data[5,6] on $NiSiF_6 \cdot {}_6H_2O$ at low temperatures are reasonably well described by a single-ion spin Hamiltonian of the form

$$\mathcal{H} = g_\parallel \mu_B H_z S_z + g_\perp \mu_B (H_x S_x + H_y S_y) + DS_z^2 , \qquad (1)$$

with $S = 1$, $g_\parallel \approx g_\perp = 2.24$ and $D = -0.16k$. Thus the ${}^3A_{2g}$ ground state of the octahedral $[Ni(H_2O)_6]^{2+}$ complex is split under the combined actions of the trigonal distortion of the crystal-field and spin-orbit coupling into a lower doublet and an upper singlet separated, below 4 K, by $|D| = 0.16k$. Evidence of a weak ferromagnetic interaction among Ni^{2+} ions, which form a nearly-simple-cubic lattice, was also extracted from EPR linewidth data.[7,8] Magnetic and thermal measurements[5] subsequently revealed magnetic ordering below a Curie temperature of ~0.15 K.

More recently the structural prototype, $NiSnCl_6 \cdot 6H_2O$, itself has been studied at low temperatures. It is possible to describe magnetic, thermal[9] and EPR[10] data below 4.2 K in first approximation with Eq. (1) assuming that $g_\parallel \approx g_\perp \approx 2.25$ and $D \approx +0.6k$. Thus the basic spin triplet is split into a lower singlet and an upper doublet, in marked contrast with the fluosilicate. In addition, it has been found possible[9] to improve the fit of the data substantially by introducing a weak coupling between Ni^{2+} ions of antiferromagnetic sign, i.e., opposite that in the fluosilicate.

We have also found[11] singlet ground states ($D > 0$) and evidence of antiferromagnetic spin coupling in several other salts of the $NiSnCl_6 \cdot 6H_2O$ structure with the formula $NiMX_6 \cdot 6H_2O$ where $M^{4+} = Pt^{4+}$, Pd^{4+} and $X^- = Cl^-, Br^-, I^-$. It is, therefore, reasonable to ask whether or not the doublet ground state ($D < 0$) and ferromagnetic coupling in the fluosilicate are anomalous or perhaps characteristic of those compounds containing the fluoride ion. To examine this question, we have prepared crystals of $NiZrF_6 \cdot 6H_2O$, $NiTiF_6 \cdot 6H_2O$, and $NiSnF_6 \cdot 6H_2O$ all of which appear to exhibit, at least at room temperature, the $NiSnCl_6 \cdot 6H_2O$ structure. In this paper, we report the measurement, at temperatures above ~0.05 K of the low-field magnetic susceptibilities and heat capacity of $NiZrF_6 \cdot 6H_2O$. As we shall see, it does resemble the fluosilicate in that $D < 0$ and the net spin coupling is ferromagnetic. However, $|D|$ proves to be larger in the fluozirconate by more than an order of magnitude, a fact which has quite interesting consequences.

EXPERIMENTAL DETAILS

Nickel fluozirconate hexahydrate was prepared by dissolving equimolar quantities of NiO and ZrO_2 in hot hydrofluoric acid and mixing the two

solutions in a polyethylene beaker. On cooling, the solution yields tiny crystals which are then filtered out, dissolved in water and allowed to recrystallize by slow evaporation at room temperature. The addition of excess HF prevents precipitation of oxides and promotes the growth of large crystals. These are green in color, elongated parallel to the trigonal axis, and stable in air. X-ray powder photographs[12] indicated that the structure is rhombohedral with unit-cell parameters $a = 6.52$ Å and $\alpha = 96°18'$. These results and the external morphology of the crystals suggest strongly that $NiZrF_6 \cdot 6H_2O$ crystallizes in the $NiSnCl_6 \cdot 6H_2O$ structure.

Most of the measurements to be described were performed in a ^{3}He-^{4}He dilution cryostat at temperatures between ~0.05 and 4.2 K. Magnetic susceptibilities were determined by a mutual inductance technique[13] at a frequency of 70 Hz. Three matched mutual inductances thermally anchored to the 1-K reservoir of the dilution refrigerator and symmetrically arranged with respect to the mixing chamber were used. These enabled us to measure in one experiment the susceptibilities of $NiZrF_6 \cdot 6H_2O$ along and perpendicular to the trigonal axis, as well as the susceptibility of a cerium magnesium nitrate (CMN) thermometric sample. All three specimens were mounted inside but isolated from their respective coils and thermally linked by bundles of insulated copper wires to the mixing chamber.

The data reported were taken on two crystals shaped into ellipsoids of revolution with the major axes parallel and perpendicular to the trigonal axis. The specimen used to measure $\chi_\parallel$ weighed 0.2122 ± 0.0005 g and had semiaxes $a = 3.6$ mm and $b = c = 2.3$ mm. The calculated demagnetizing factor was $\mathfrak{D} = 2.82$. $\chi_\perp$ was measured with a crystal weighing 0.2149 ± 0.0005 g and having semiaxes $a = 3.6$ mm and $b = c = 2.4$ mm. The susceptibility of each of these specimens was first measured by the ac method between 0.3 and 4.2 K in a liquid-^{3}He-cooled cryostat. In those preliminary experiments, the $NiZrF_6 \cdot 6H_2O$ crystals as well as a CMN standard could be successively inserted into the same mutual inductance at each temperature. Thus $\chi_\parallel$ and $\chi_\perp$ could be determined relative to the known susceptibility[14] of CMN. Data taken in the dilution cryostat, in which no such interchange was possible, were subsequently normalized to the values determined in this way above 0.3 K.

In order to measure heat capacities, the mutual inductance assembly was removed from the dilution cryostat and replaced with a calorimetric insert.[15] This consists of a supporting mount carrying the single-crystal specimen (3.5 cm $\times 1.5$ cm $\times 0.5$ cm weighing 3.54 g), its suspension, and a bundle of 3000 #40 Cu wires linking it to the mixing chamber via a pincerstype mechanical heat switch. A Speer 220-Ω $\frac{1}{2}$-W carbon resistor and a heater winding are attached to the wire heat link. The carbon thermometer was calibrated, with the heat switch closed, against a CMN thermometer mounted directly on the mixing chamber. The CMN thermometer calibration constant was in turn determined above 0.5 K by means of an encapsulated germanium thermometer also attached to the mixing chamber. The Ge thermometer had been previously calibrated against the vapor pressure of liquid ^{3}He in another cryostat.

The thermometer calibration procedure, beginning with the establishment of the constant for the magnetic thermometer, was carried out after each warming of the cryostat to room temperature. Extrapolating the magnetic scale to 0.050 K, the carbon resistor and magnetic thermometer were compared at about twenty points between 0.05 and 4.2 K. These R-T data were fitted with an expression of the form

$$\left(\frac{\log R}{T}\right)^{1/2} = A + B(\log R) + C(\log R)^2 + D(\log R)^3 . \quad (2)$$

The rms deviation of the observed from the calculated temperatures was typically about 1%. In order to keep power dissipation in the thermometer at acceptably low levels ($< 10^{-12}$ W at 50 mK), it was necessary to operate the Wheatstone bridge measuring circuit at low currents and to measure the imbalance signal with a phase sensitive detector (PAR Model 121).

The lower end of the calorimeter insert and its surrounding vacuum jacket fit into the bore (4.6 cm diameter) of a Nb-Zr superconducting solenoid capable of producing fields at the specimen up to ~57 kOe. In the present experiments, the trigonal axis of the crystal (long axis of the specimen) was aligned with the field to within ~±3°. The carbon thermometer is situated outside the solenoid and was not subjected to fields large enough to produce significant magnetoresistive effects. All heat-capacity data reported below were obtained by the discontinuous heating (heat pulse) method.

RESULTS AND DISCUSSION

Figure 1 shows the susceptibilities of $NiZrF_6 \cdot 6H_2O$ measured parallel and perpendicular to the trigonal axis between ~0.5 and ~4 K in the ^{3}He cryostat. Also shown over the same interval are values of the susceptibility of a spherical sample of compressed powder measured in the same cryostat. A curve calculated from the single-crystal data according to the relation χ_{powder}

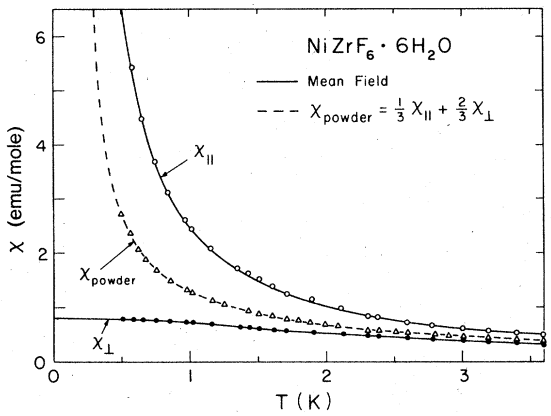

FIG. 1. Magnetic susceptibilities of powder and single-crystal (parallel and perpendicular to the trigonal axis) specimens of $NiZrF_6 \cdot 6H_2O$. Solid curves are calculated for mean-field model with $D/k = -3.00$ K, $g = 2.36$, and $n = +0.06$ mole/emu.

$= \frac{1}{3}\chi_{\parallel} + \frac{2}{3}\chi_{\perp}$ is seen to fit the powder values quite well. This is consistent with the persistence in this region of the uniaxial anisotropy which characterizes the crystal at room temperature.

It is instructive to analyze the data of Fig. 1 in a preliminary way before presenting the results of measurements at lower temperatures. If the interactions among Ni^{2+} ions are ignored, then a plausible model for this system is given by the single-ion-spin Hamiltonian of Eq. (1) with $S = 1$ and the z direction along the trigonal axis of the crystal. The energy eigenvalues of Eq. (1) are for $\vec{H} \parallel \vec{z}$,

$$W_1 = D - g_{\parallel}\mu_B H\,, \quad W_2 = D + g_{\parallel}\mu_B H\,, \quad W_3 = 0 \tag{3}$$

and for $\vec{H} \perp \vec{z}$,

$$W_1 = D\,, \quad W_2 = \tfrac{1}{2}[D - (D^2 + 4g_{\perp}^2\mu_B^2 H^2)^{1/2}]\,,$$
$$W_3 = \tfrac{1}{2}[D + (D^2 + 4g_{\perp}^2\mu_B^2 H^2)^{1/2}]\,. \tag{4}$$

Using these sets of field-dependent levels it is a straightforward matter to form partition functions and calculate, in the zero-field limit, the susceptibilities for N noninteracting ions. These are

$$\chi_{\parallel}^0 = \frac{2Ng_{\parallel}^2\mu_B^2}{kT}\,\frac{1}{e^{D/kT} + 2}\,, \tag{5}$$

$$\chi_{\perp}^0 = \frac{2Ng_{\perp}^2\mu_B}{D}\,\frac{e^{D/kT} - 1}{e^{D/kT} + 2}\,. \tag{6}$$

From the theory of the spin Hamiltonian[16] one finds

$$g_{\parallel} - g_{\perp} = 2D/\lambda\,. \tag{7}$$

Since for the $[Ni(H_2O)_6]^{2+}$ complex, the spin-orbit parameter λ is ~ -270 cm^{-1},[17] and $|D|$ is typically ~ 1 cm^{-1}, the difference $g_{\parallel} - g_{\perp}$ is usually too small to be easily detected in susceptibility measurements. Except where otherwise noted, we shall assume $g_{\parallel} = g_{\perp} = g$.

From Fig. 1, we see that $\chi_{\parallel} > \chi_{\perp}$ over the whole temperature range. From Eqs. (5) and (6) one finds

$$\chi_{\parallel}^0 / \chi_{\perp}^0 = (D/kT)/(e^{D/kT} - 1)\,,$$

which is ≥ 1 for $D < 0$. Thus for $NiZrF_6 \cdot 6H_2O$, $D < 0$ and the basic spin triplet is split into a lower doublet and an upper singlet, as is the case for $NiSiF_6 \cdot 6H_2O$. In order to estimate the magnitude of this zero-field splitting and of the g factor we have fitted Eqs. (5) and (6) to the data of Fig. 1 in various ways. A least-squares fit of Eq. (6) to $\chi_{\perp}$ yields $D \approx -2.7k$ and $g \approx 2.4$, for example. Those parameters inserted in Eq. (5) give reasonable fit of $\chi_{\parallel}$ at the highest temperatures but the model fails quantitatively as the temperature falls.

Guided by earlier experience[9] with $NiSnCl_6 \cdot 6H_2O$, we have tried to improve the fit of these data by introducing interaction among Ni^{2+} ions in a simplified mean-field approximation. The magnetic field H in Eq. (1) is replaced by an effective field which is the sum of the applied field and a term proportional to the magnetization $\vec{M}$ of the specimen, i.e.,

$$\vec{H}_{eff} = \vec{H} + n\vec{M}\,. \tag{8}$$

For weak effective fields, $\vec{M} = \chi^0\vec{H}_{eff}$, where χ^0 is given either by Eq. (5) or Eq. (6). For weak applied fields the temperatures where no spontaneous order occurs, we can also write $\vec{M} = \chi\vec{H}$ where χ is the initial susceptibility of a system of interacting ions. Thus

$$\chi = \vec{M}/\vec{H} = \chi^0(1 + n\chi)\,,$$

and either

$$\chi_{\parallel} = \chi_{\parallel}^0/(1 - n\chi_{\parallel}^0) \tag{9}$$

or

$$\chi_{\perp} = \chi_{\perp}^0/(1 - n\chi_{\perp}^0)\,. \tag{10}$$

A least-squares fitting of all of the data of Fig. 1 using Eqs. (9) and (10) and allowing D, g, and n to vary, yields the parameters $D/k = -3.00$ K, $g = 2.36$, and $n = +0.06$ mole/emu. The solid curves shown in Fig. 1 are calculated with these parameters and reproduce the data quantitatively. The fact that the mean-field constant $n > 0$ indicates that the net effective spin coupling in $NiZrF_6 \cdot 6H_2O$ is ferromagnetic as it is in $NiSiF_6 \cdot 6H_2O$. Quite striking, however, is the magnitude of D, which is larger by a factor of almost 20 than the zero-field splitting in the fluosilicate.

An estimate of the temperature-independent Van

Vleck susceptibility can be made using the g factor as determined above. Adding to the spin Hamiltonian, Eq. (1), the quadratic Zeeman term[16] previously omitted, the Van Vleck contribution to the paramagnetic susceptibility is easily derived. It may be written in the form

$$\chi_{VV} = (N_0\mu_B^2/\lambda)(2-g). \tag{11}$$

Taking $\lambda \approx -270$ cm^{-1} and $g = 2.36$, one finds $\chi_{VV} = 3.53\times10^{-4}$ emu/mole. The temperature-independent diamagnetic contribution may be estimated from the tabulated values[18] for the component ions and ligands to be -1.67×10^{-4} emu/mole. The net temperature-independent susceptibility is thus $+1.86\times10^{-4}$ emu/mole and is negligible in the temperature region of interest.

The signs and magnitudes of D and the mean-field coupling constant in $NiZrF_6\cdot6H_2O$ inferred from the simple analysis of the susceptibilities at relatively high temperatures suggest the occurrence of ferromagnetic ordering near 0.1 K. This is confirmed by measurements of $\chi_\parallel$ and $\chi_\perp$ carried out in the ^{3}He-^{4}He dilution refrigerator down to ~0.05 K. The data are shown in Fig. 2 where $\chi_\parallel$ and $\chi_\perp$ are plotted on different scales. $\chi_\parallel$ rises rapidly to a distinct peak at ~0.16 K which is presumably the Curie point T_C. The much smaller peak exhibited at the same temperature by $\chi_\perp$ could easily be the result of slight specimen misalignment. As the transition temperature was approached from above, not only did $\chi_\parallel$ become very large, but it also developed a large loss component. The resultant power dissipation in the specimen caused warming of the mixing chamber of the dilution refrigerator and made measurement of $\chi_\parallel$ near T_C difficult. Such losses are suggestive of the onset of some form of ferromagnetic order.

Of particular significance is the magnitude of $\chi_\parallel$ below T_C. At the lowest temperature, ~0.058 K, we find $\chi_\parallel$, expressed in emu/cm^3, nearly constant at 0.352. The calculated demagnetization factor for the ellipsoidal specimen is $\mathfrak{D} = 2.82$. Thus $1/\mathfrak{D} = 0.354 \simeq \chi_\parallel$, as expected for a ferromagnet which has no remanence. In such a material, a small field H_{app} applied along the easy direction is exactly compensated by the demagnetizing field $-\mathfrak{D}M$, so that the internal field $H_{int} = H_{app} - \mathfrak{D}M = 0$. This occurs when the measured susceptibility $\chi = (\partial M/\partial H_{app})_T = 1/\mathfrak{D}$. In $NiZrF_6\cdot6H_2O$, the single-ion anisotropy DS_z^2, with $D \ll 0$, establishes the trigonal axis as the easy direction and the plane perpendicular to that axis as a "hard" plane. The large negative value of D insures that $\chi_\perp$ is much smaller than $\chi_\parallel$ at and below T_C as well as above it.

Let us consider now the results of heat-capacity measurements on $NiZrF_6\cdot6H_2O$ above ~0.09 K in zero applied field. Figure 3 shows the magnetic contribution to the heat capacity C_P(mag) as a function of temperature below 4.2 K. A very sharp cooperative peak at $T_C = 0.164 \pm 0.002$ K marks the Curie point. It is followed by a well-resolved Schottky anomaly ($T_{max} \sim 1.5$ K) associated with the thermal population of the single-ion excited singlet. Separation of C_P(mag) from the measured total heat capacity of the specimen and its calorimetric addenda was effected approximately by fitting those data in the interval 2.6 to 4.2 K with an expression of the form

$$C_P = aT + bT^3 + C^0(\text{mag}). \tag{12}$$

The first two terms are used to represent the

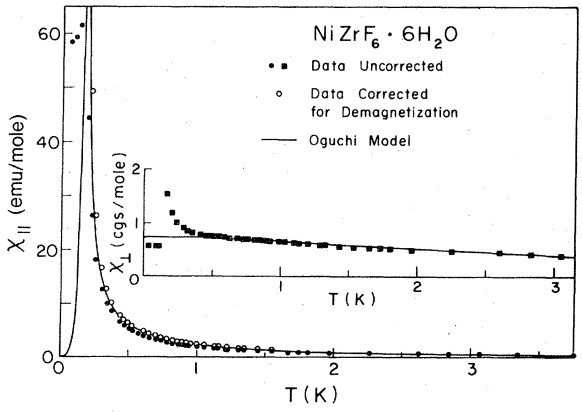

FIG. 2. Magnetic susceptibilities parallel and perpendicular to the trigonal axis of $NiZrF_6\cdot6H_2O$ down to 0.05 K. Solid curves calculated for Oguchi model with $D/k = -3.00$ K, $g = 2.33$ K, and $zJ/k = +0.084$ K. $T_C = 0.164$ K.

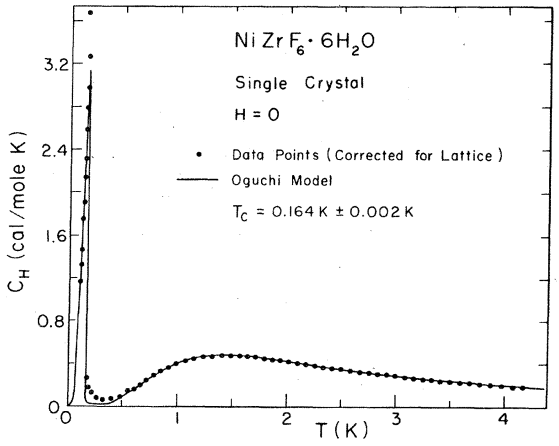

FIG. 3. Magnetic heat capacity of $NiZrF_6\cdot6H_2O$ crystal in zero applied field. Solid curve calculated for Oguchi model with $D/k = -3.14$ K and $zJ/k = +0.082$ K.

free-electron and lattice contributions of the addenda as well as the lattice part of the specimen heat capacity. The third term is the heat capacity of N noninteracting Ni^{2+} ions calculated with the energy levels of Eqs. (3) for $H=0$, namely,

$$C^0(\text{mag}) = 2Nk\left(\frac{D}{kT}\right)^2 \frac{e^{D/kT}}{(e^{D/kT}+2)^2}. \tag{13}$$

A good fit was obtained with $D/k=-3.14$ K. The difference $C_P - C^0(\text{mag}) = aT + bT^3$, was then assumed to approximate nonmagnetic contributions to the total measured heat capacity over the entire range, 0.09 to 4.2 K. This correction amounted to 0.04% of the raw values at 0.2 K, 1.4% at 0.85 K, 6.3% at 2 K, and 50% at 4.1 K. The values of C_P(mag) shown in Fig. 3 are the result of subtracting off these nonmagnetic correction terms.

The fully resolved Schottky and cooperative anomalies of Fig. 3 emphasize graphically an important property of $NiZrF_6 \cdot 6H_2O$ already inferred from the fitting of susceptibility data well above T_C, namely, that the interactions among Ni^{2+} ions are weak in comparison with separation $|D|$ of the single-ion doublet ground state and excited singlet. At T_C the singlet ($m_s=0$) is not thermally populated and the Ni^{2+} spins have essentially the $m_s=\pm 1$ character of the doublet. In other words, they can point in the $\pm z$ directions and thus behave as Ising spins. However, a comparison of the heat-capacity data for $0.6 < T/T_C < 2$ with theoretical estimates[19] for an Ising model on a simple cubic lattice with nearest-neighbor interaction reveals significant systematic discrepancies. At the same time, the abrupt, possibly discontinuous, drop in C_P at T_C together with the relatively insignificant short-range-order tail above T_C are suggestive of a simple second-order transition describable by mean-field theory.

In order to examine further the possibility of mean-field behavior in $NiZrF_6 \cdot 6H_2O$, we have fitted the heat-capacity and susceptibility data with two mean-field models. The first is of the simple kind previously described. Because of the small but noticeable tail exhibited by C_P above T_C, it was considered worthwhile also to use a model which, to some extent, incorporates the effects of short-range order. The simplest of these is the Oguchi model[20] in which interactions between pairs of neighboring magnetic ions are treated exactly and the interaction of the pair with the rest of the lattice is approximated by a mean field. The pair, rather than some larger cluster such as an ion and all its nearest neighbors, is chosen for exact treatment because of its simplicity and tractability and generally has no structural significance. This method treats short-range order effects only approximately and usually underestimates their magnitude. Since the two procedures yield very similar results and the Oguchi model for $S=1$ with uniaxial anisotropy is relatively unfamiliar, we shall limit our discussion to that case.

The Hamiltonian of any two nearest-neighbor spins $\vec{S}_i$ and $\vec{S}_j$ interacting with one another and with their other nearest neighbors via isotropic exchange is

$$\mathcal{H}_{\text{pair}} = D(S_{iz}^2 + S_{jz}^2) - 2J\vec{S}_i \cdot \vec{S}_j - 2J\left(\sum_k \vec{S}_k \cdot \vec{S}_i + \sum_l \vec{S}_l \cdot \vec{S}_j\right). \tag{14}$$

Here the indices k and l refer to all nearest neighbors of spin i (except spin j) and of spin j (except spin i), respectively. Oguchi replaces the operators $\vec{S}_k$ and $\vec{S}_l$ by their thermal average expectation values $\langle \vec{S} \rangle$ and notes that only $\langle \vec{S}_z \rangle$ does not vanish. With these substitutions and adding a magnetic field $H_\parallel$ in the z direction, the pair Hamiltonian becomes

$$\mathcal{H}_{\text{pair}} = D(S_{iz}^2 + S_{jz}^2) - 2J\vec{S}_i \cdot \vec{S}_j - 2J(z-1)\langle S_z \rangle (S_{iz} + S_{jz}) + g\mu_B H_\parallel (S_{iz} + S_{jz}), \tag{15}$$

where z is the total number of nearest neighbors to a given magnetic ion. Since the expectation values of S_{iz} and S_{jz} should be the same as those of their nearest-neighbor spins, $\langle S_z \rangle$ should satisfy in a self-consistent way the relation

$$2\langle S_z \rangle = \langle S_{iz} + S_{jz} \rangle = \text{Tr}(S_{iz} + S_{jz}) e^{-\beta \mathcal{H}_{\text{pair}}} / \text{Tr} e^{-\beta \mathcal{H}_{\text{pair}}} \tag{16}$$

where $\beta = 1/kT$. The magnetization of the specimen along the z axis is related to $\langle S_z \rangle$ by the equation

$$M_\parallel = Ng\mu_B \langle S_z \rangle. \tag{17}$$

Thus $\mathcal{H}_{\text{pair}}$ can be rewritten

$$\mathcal{H}_{\text{pair}} = D(S_{iz}^2 + S_{jz}^2) - 2J\vec{S}_i \cdot \vec{S}_j + g\mu_B H_{\text{eff}} (S_{iz} + S_{jz}), \tag{18}$$

where

$$H_{\text{eff}} = H_\parallel - \frac{2J(z-1)}{Ng^2\mu_B^2} M_\parallel. \tag{19}$$

Equations (18) and (19) show explicitly the action on each ion pair of an applied field $H_\parallel$ as well as of a mean-field proportional to the magnetization of the sample.

The eigenvalues and eigenvectors of H_{pair} for $S_i = S_j = 1$ are found to be:

$$E_1 = D + J - [(D+J)^2 + 8J^2]^{1/2};$$
$$\phi_1 = (E_1^2 + 8J^2)^{-1/2} \times \left[-2\sqrt{2}J\,|0,0\rangle + \frac{E_1}{\sqrt{2}}(|+,0\rangle + |-,+\rangle)\right];$$
$$E_2 = D + 2J + X; \quad \phi_2 = \frac{1}{\sqrt{2}}(|+,0\rangle + |0,+\rangle);$$
$$E_3 = D - 2J - X; \quad \phi_3 = \frac{1}{\sqrt{2}}(|0,-\rangle + |-,0\rangle);$$
$$E_4 = D + 2J + X; \quad \phi_4 = \frac{1}{\sqrt{2}}(|+,0\rangle - |0,+\rangle);$$
$$E_5 = D + 2J - X; \quad \phi_5 = \frac{1}{\sqrt{2}}(|0,-\rangle - |-,0\rangle); \qquad (20)$$
$$E_6 = D + J + [(D+J)^2 + 8J^2]^{1/2};$$
$$\phi_6 = (E_9^2 + 8J^2)^{-1/2} \times \left[-\sqrt{2}J\,|0,0\rangle + E_9\frac{1}{\sqrt{2}}(|+,-\rangle + |-,+\rangle)\right];$$
$$E_7 = 2(D+J); \quad \phi_7 = \frac{1}{\sqrt{2}}(|+,-\rangle - |-,+\rangle);$$
$$E_8 = 2(D - J + X); \quad \phi_8 = |+,+\rangle;$$
$$E_9 = 2(D - J - X); \quad \phi_9 = |-,-\rangle;$$

where $X = g\mu_B H_\parallel - 2(z-1)J\langle S_z\rangle = g\mu_B H_{\text{eff}}$.

As is evident from Eqs. (16) and (17), the magnetization may be calculated in a straightforward way from the pair partition function $Z = \mathrm{Tr}(e^{-\beta H_{\text{pair}}}) = \sum_i e^{-\beta E_i}$, according to the relation $M = (1/\beta)(1/Z)(\partial Z/\partial H)$. The result is a transcendental equation which must be solved self-consistently. For comparison with our experiments, it was also necessary to obtain $\chi = (\partial M/\partial H)|_{H=0}$. Using Eqs. (20), we have calculated $\chi_\parallel$. For $\vec{H} \perp \vec{z}$, the diagonalization of the pair Hamiltonian was carried out,[13] in part numerically, and $\chi_\perp$ computed in an analogous way.

The best fit of $\chi_\parallel$ and $\chi_\perp$ with the Oguchi model was obtained for $D/k = -3.00$ K, $g = 2.33$, and $zJ/k = +0.084$ K. The solid curves of Fig. 2 show the results of this fit. They have been calculated for long needle-shaped specimens with the needle axis $\parallel$ and $\perp$ to the z direction, i.e., with no demagnetizing effects. Where the measured susceptibilities (solid points in Fig. 2) become large above T_C they must be corrected to this geometry for comparison with theory. This has been done using the familiar relation

$$1/\chi_\infty = 1/\chi_{\text{meas}} - \mathfrak{D}/V_{\text{mole}}. \qquad (21)$$

Such corrected data points are shown as open circles in Fig. 2. At $T_C = 0.164$ K the model begins to exhibit spontaneous magnetization. This agrees with both the $\chi_\parallel$ data and the C_P data of Fig. 3. Note that the theoretical value of $\chi_\parallel$ drops to zero below T_C because the needle-like specimen for which it is calculated consists of a single domain. The values of D and g obtained with the Oguchi model are essentially the same as those given in the simple mean-field model as indicated above.

The internal energy of the Oguchi model of a crystal with N magnetic ions was obtained by calculating the thermal average expectation values of each of the operators appearing in $\mathfrak{IC}_{\text{pair}}$ [Eq. (15)], multiplying them by the appropriate numerical factors and adding all of the contributions. The result is

$$U = \tfrac{1}{2}N[D\langle S_{iz}^2 + S_{jz}^2\rangle - 2J\langle \vec{S}_i \cdot \vec{S}_j\rangle + g\mu_B H_\parallel \langle S_{iz} + S_{jz}\rangle - \tfrac{1}{2}(z-1)J\langle S_{iz} + S_{jz}\rangle^2]. \qquad (22)$$

It differs from $\frac{1}{2}N\langle \mathfrak{IC}_{\text{pair}}\rangle$ by the factor $\frac{1}{2}$ in the mean-field (last) term which is introduced to avoid counting twice the interactions of spins belonging to neighboring pairs. The averages in Eq. (21) were determined in the usual way, e.g.,

$$\langle \vec{S}_i \cdot \vec{S}_j\rangle = \frac{\mathrm{Tr}[(\vec{S}_i \cdot \vec{S}_j)e^{-\beta H_{\text{pair}}}]}{\mathrm{Tr}(e^{-\beta H_{\text{pair}}})}.$$

The heat capacity was then calculated by differentiating the internal energy, $C_H(T) = (\partial U(T,H)/\partial T)_H$.

It should be noted from Eq. (22) that when $\langle S_{iz} + S_{jz}\rangle$ is zero, i.e., above T_C for $H = 0$, only one of the z nearest-neighbor interactions of a given ion is taken into account. This is an unrealistic feature of the model which leads to an underestimate of the short-range-order contribution to the heat capacity in zero field. A better representation of the observations in that region could be obtained by taking as the interaction contribution to the internal energy the expression[21] $-NJz\langle S_i \cdot S_j\rangle$. This choice leads, however, to an incorrect result for the difference in magnetic entropy between the completely ordered and disordered states, $\Delta S = \int_0^\infty C_H/T\,dT$. In contrast, Eq. (22) ultimately yields the expected value, $Nk\ln 3$, for this entropy difference and is consistent with the pair Hamiltonian, Eq. (15).

We have fitted the Oguchi model to the magnetic part of the heat capacity of $NiZrF_6 \cdot 6H_2O$ by a least-squares procedure in which D and J were allowed to vary. The theoretical result is shown as a solid curve in Fig. 3. Agreement with the experimental data is quite gratifying. The best values for the fitted parameters are $D/k = -3.14$ K, and $zJ/k = +0.0816$ K while the calculated Curie point is $T_C = 0.164$ K. The agreement with the corresponding values obtained by fitting the susceptibility data, $D/k = -3.00$ K and $zJ/k = 0.084$ K, is excellent. The limitations of the model are

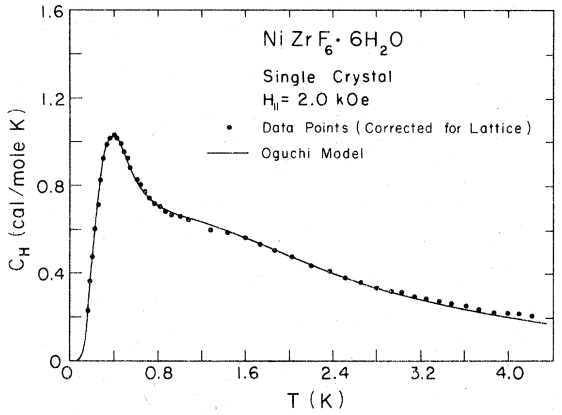

FIG. 4. Magnetic heat capacity of $NiZrF_6 \cdot 6H_2O$ with $H_{||} = 2$ kOe. Solid curve calculated for Oguchi model with $D/k = -3.14$ K, $g = 2.36$, and $zJ/k = +0.082$ K.

evident just above T_C where, as expected, it underestimates the magnitude of the heat-capacity tail by a factor of about $1/z$ or $\frac{1}{6}$. At or slightly below T_C, the data rise above the calculated values. Possible implications of this behavior will be mentioned below.

An interesting test of the relevance of a mean-field model to this system is provided by a series of measurements of the heat capacity of a single crystal of $NiZrF_6 \cdot 6H_2O$ with a field of 2000 Oe applied parallel to the trigonal axis. The sample and its addenda are the same as those used in the zero-field measurements. The combined lattice-addenda correction determined in zero field was therefore subtracted from the measured total heat capacity to yield the magnetic part shown in Fig. 4. The applied field in this case is small in comparison with $D/g\mu_B \sim 19.6$ kOe and yet large enough in comparison with M/V that the heat capacity in constant applied field $C_{H_{app}}$ is essentially the heat capacity in constant internal field C_H. As Griffiths[22] has shown, the sharp zero-field cooperative anomaly at T_C is replaced in this case by the rounded and broadened anomaly predicted for most model ferromagnets by theories of in-field behavior which ignore demagnetizing effects. This behavior, as well as modification of the upper Schottky maximum, are dramatically illustrated in Fig. 4.

We have fitted the data of Fig. 4 with the Oguchi model using the values $D/k = -3.14$ K and $zJ/k = +0.082$ K, determined from the zero-field heat-capacity results and $g = 2.36$ as required by the low-field susceptibility measurements. Only the internal field was varied in the least-squares fitting procedure. The solid curve in Fig. 4 shows the theoretical result for an internal field $H_{int} = 1894$ Oe. The ability of the mean-field model to reproduce the observations is very striking. The difference of ~100 Oe between the applied and internal fields represents a demagnetizing field. The specimen crystal was elongated along the c axis and its edges had been rounded off, but it was not ellipsoidal. The internal magnetic field is thus probably somewhat nonuniform. Assuming, however, an ellipsoidal sample of the same extremal dimensions, one estimates at 0.1 K a demagnetizing field of ~70 Oe, which is reasonably close to the empirical value.

We turn now to consideration of the possible origin of mean-field behavior in $NiZrF_6 \cdot 6H_2O$. As was emphasized earlier, the large separation of the doublet ground state from the excited singlet in this salt gives it pronounced Ising character. It was also noted than an Ising model with nearest-neighbor interaction alone did not reproduce the data very well. It has been shown,[23] however, that an Ising ferromagnet in the limit in which all spins interact equally with one another exhibits mean-field behavior. The general case in which interactions are ferromagnetic, of infinite range, and decrease with interspin separation according to a power law, has also been studied.[24] In three-dimensional systems of this type, mean-field behavior is expected if the interaction falls off slowly enough with distance.

The inverse cube law of the dipolar interaction satisfies this criterion. However, the angular dependence of the sign of the dipolar coupling renders it not purely ferromagnetic so that, in general, it need not lead to mean-field behavior. A system of Ising spins with dipolar interaction proves to be a special case of particular interest. Larkin and Khmel'nitskii[25] and Fisher and Aharony[26] have shown that the critical properties of the dipolar Ising ferromagnet in zero field are mean-field-like but with corrections involving $|\ln t|$ where $t \equiv T/T_C - 1$. In general, the logarithmic corrections are difficult to detect. Except under high-temperature resolution very close to T_C many properties of dipolar Ising ferromagnets will appear to be essentially mean-field-like. Aharony[27] has also considered the critical behavior of uniaxial ferromagnets with both exchange and dipolar interactions. He finds a crossover to the dipolar regime at a value of t which grows with increasing admixture of dipolar coupling.

These results suggest that what we are observing in $NiZrF_6 \cdot 6H_2O$ may be the approximate mean-field behavior of an Ising ferromagnet in which dipolar interactions are important. This interpretation is quite consistent with the low value of T_C and the structure of the salt. It implies, of course, that the quantity zJ determined by fitting the Oguchi model to the data must be regarded as

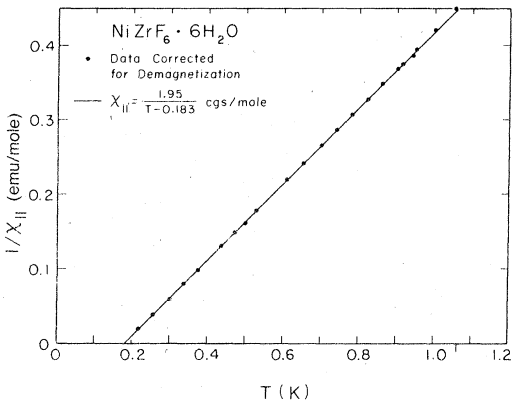

FIG. 5. Reciprocal of $\chi_{\parallel}$ for $NiZrF_6 \cdot 6H_2O$ vs temperature above T_C.

a measure of the net effect of interactions of several kinds and not of nearest-neighbor exchange alone.

In order to estimate semiquantitatively the relative importance of dipolar and exchange interactions in this salt, it is useful to examine the behavior of $\chi_{\parallel}$ in the paramagnetic region. Correcting the data for demagnetization effects, according to Eq. (21), we plot $1/\chi_{\parallel}^{\infty}$ versus T in an interval in which only the doublet ground state of the single Ni^{2+} ion is significantly populated, $T \lesssim 1.1$ K (Fig. 5). Here one may reasonably ascribe to the ion an anisotropic moment with effective spin $S' = \frac{1}{2}$. The data are well described by a Curie-Weiss law $\chi_{\parallel}^{\infty} = C_{\parallel}/(T - \theta_{\parallel})$ where $C_{\parallel} = 1.95 \pm 0.02$ cgs K/mole and $\theta_{\parallel} = 0.183 \pm 0.003$ K. Assuming $S' = \frac{1}{2}$, the Curie constant $C_{\parallel} = N_0 g_{\parallel}'^2 \mu_B^2 S'(S'+1)/3k$ yields $g_{\parallel}' = 4.526$.

The leading terms of the high-temperature series expansions of the thermodynamic properties of a system of ions with dipolar interaction have been calculated by Van Vleck.[28] Daniels[29] has extended this work to include ions with anisotropic moments. The dipolar contribution Δ to the Weiss constant θ obtained in these calculations is often written approximately as a sum of two parts

$$\Delta = \Delta^{\mathrm{sph}} + \tfrac{4}{3}\pi \frac{C}{V_{\mathrm{mole}}} . \tag{23}$$

Δ^{sph} is the result of the interaction of ions j at all lattice sites within a spherical volume inside the sample with the ion i at its center. For ions with spin $\frac{1}{2}$ and $\vec{H} \parallel \vec{z}$ Daniels finds

$$\Delta_{\parallel}^{\mathrm{sph}} = \frac{g_{\parallel}^2 \mu_B^2}{4k} \sum_j \frac{3z_{ij}^2 - r_{ij}^2}{r_{ij}^5} , \tag{24}$$

where the summation is carried out inside the sphere, the radius having been taken large enough that the contribution of the next spherical shell is negligible. The rest of the ions in the needlelike crystal are replaced by a magnetizable continuum with poles on the surface of the spherical hole which produce the so-called Lorentz field at i and contribute to Δ the term $4\pi C/3V_{\mathrm{mole}}$.

The sum in Eq. (24) has been evaluated within a sphere of radius ~328 Å by computer. With $g_{\parallel}' = 4.526$, we find $\Delta_{\parallel}^{\mathrm{sph}} = -0.005\,3$ K, the small magnitude reflecting the approximately simple cubic nature of the spin lattice. Taking $C_{\parallel} = 1.95$ emu K/mole and $V_{\mathrm{mole}} = .167.4$ cm^3, the Lorentz term is $4\pi C_{\parallel}/3V_{\mathrm{mole}} = +0.0488$ K. Thus $\Delta = +0.0435$ K.

The leading terms of the high-temperature expansion of the susceptibility of a system of ions with nearest-neighbor isotropic exchange interaction $(-2J'\vec{S}_i' \cdot \vec{S}_j')$ take the form of the Curie-Weiss law.[30] If a given ion of effective spin $S' = \frac{1}{2}$ interacts with z equivalent nearest neighbors, the Weiss constant is $zJ'/2k$. Assuming additivity of the exchange and dipolar contributions, as is reasonable in this approximation, the Weiss constant becomes

$$\theta_{\parallel} = \Delta + \frac{zJ'}{2k} . \tag{25}$$

Inserting the measured $\theta_{\parallel}$ and calculated Δ values, we find $zJ'/2k = +0.183 - 0.044 = 0.139$ K. Transforming back into an $S = 1$ formalism, this becomes $zJ/k = +0.104$ K. This is not very different from the effective coupling estimated with the Oguchi model, namely, $zJ/k = +0.084$ K. Comparing $\theta_{\parallel}$ and Δ, we see that the dipolar part amounts to 24% of the measured Weiss constant and is thus almost one-third the nearest-neighbor exchange contribution in magnitude.

These estimates indicate that dipolar interaction in $NiZrF_6 \cdot 6H_2O$ provides a substantial part of the interionic spin coupling. It seems to add enough long-range character to that coupling to make the properties of this salt distinctly mean-field-like rather than those of a simple nearest-neighbor Ising ferromagnet. The latter quality is not completely obscured, however, as is evident in the zero-field heat capacity (Fig. 3) just above T_C, where a small short-range-order "tail" occurs, or just below T_C where C_P rises slightly above the values calculated for a mean-field model.

ACKNOWLEDGMENTS

We wish to thank George Lecomte for carrying out x-ray diffraction measurements on the com-

pound investigated in this study. The work was supported in part by NSF Grant No. DMR 75-13908 and ONR Contract N 00014-75-C-0771 NR 318-026. It is based on portions of theses submitted by two of us (M.K. and D.L.M.) in partial fulfillment of the requirements for the Ph.D. degree to Carnegie-Mellon University, 1976.

[1]L. Pauling, Z. Kristallogr. 72, 482 (1930).
[2]J. Becquerel and J. van den Handel, Physica (Utr.) 6, 1034 (1939).
[3]J. Becquerel and W. Opechowski, Physica (Utr.) 6, 1039 (1939).
[4]R. P. Penrose and K. W. H. Stevens, Proc. Phys. Soc. Lond. A 63, 29 (1950).
[5]A. Ohtsubo, J. Phys. Soc. Jpn. 20, 76 (1965).
[6]E. W. Hornung, G. E. Brodale, R. A. Fisher, and W. F. Giauque, J. Chem. Phys. 45, 614 (1966).
[7]E. Ishiguro, K. Kambe, and T. Usui, Physica (Utr.) 17, 310 (1951).
[8]I. Svare and G. Seidel, Phys. Rev. 134, A172 (1964).
[9]B. E. Myers, L. G. Polgar, and S. A. Friedberg, Phys. Rev. B 6, 3488 (1972).
[10]Y. Ajiro, S. A. Friedberg, and N. S. VanderVen, Phys. Rev. B 12, 39 (1975).
[11]S. A. Friedberg, M. Karnezos, and D. Meier, *Proceedings of the Fourteenth International Conference on Low Temperature Physics, Otaniemi, Finland*, 1975, edited by M. Krusius and M. Vuorio (North-Holland, Amsterdam, 1975), p. 224.
[12]G. Lecomte (private communication).
[13]M. Karnezos, Ph.D. dissertation (Carnegie-Mellon University, 1976) (unpublished).
[14]R. P. Hudson and W. R. Hosler, Phys. Rev. 122, 1417 (1961).
[15]D. L. Meier, Ph.D. dissertation (Carnegie-Mellon University, 1975) (unpublished).
[16]M. H. L. Pryce, Proc. Phys. Soc. Lond. A 63, 25 (1950).
[17]J. Owen, Proc. R. Soc. A 227, 183 (1955).
[18]See, for example, P. W. Selwood, *Magnetochemistry*, 2nd. ed. (Interscience, New York, 1956), p. 78.
[19]A convenient tabulation of these estimates is given by H. W. J. Blöte, Ph.D. dissertation (University of Leiden, 1972) (unpublished).
[20]T. Oguchi, Prog. Theor. Phys. 13, 149 (1955).
[21]J. S. Smart, *Effective Field Theories of Magnetism* (Saunders, Philadelphia, 1966), p. 42.
[22]R. B. Griffiths, Phys. Rev. 188, 942 (1969).
[23]V. L. Ginzburg, Sov. Phys.-Solid State 2, 1824 (1961).
[24]M. E. Fisher, S.-k. Ma, and B. G. Nickel, Phys. Rev. Lett. 29, 917 (1972).
[25]A. I. Larkin and D. E. Khmel'nitskii, Sov. Phys.-JETP 29, 1123 (1969).
[26]M. E. Fisher and R. Aharony, Phys. Rev. Lett. 30, 559 (1973).
[27]A. Aharony, Phys. Lett. A 94, 313 (1973).
[28]J. H. VanVleck, J. Chem. Phys. 5, 320 (1937).
[29]J. M. Daniels, Proc. Phys. Soc. Lond. A 66, 673 (1953).
[30]W. Opechowski, Physica (Utr.) 4, 181 (1937).